

Supplement

Table S1. List of the CMIP6 models used in this study. We include every model participating in the SSP5-8.5 scenario except one (CAS-ESM-2), for which the seasonality appeared reversed because of data storage issues. For models that have several ensemble members, all of the members available for the historical period are averaged over 1980-1999, and all of the members available for the SSP5-8.5 scenario are averaged over 2080-2099.

#	Model name	#	Model name
1	ACCESS-CM2	21	GISS-E2-1-H
2	ACCESS-ESM1-5	22	HadGEM3-GC31-LL
3	AWI-CM-1-1-MR	23	HadGEM3-GC31-MM
4	BCC-CSM2-MR	24	IITM-ESM
5	CAMS-CSM1-0	25	INM-CM4-8
6	CMCC-CM2-SR5	26	INM-CM5-0
7	CMCC-ESM2	27	IPSL-CM6A-LR
8	CNRM-CM6-1	28	KACE-1-0-G
9	CNRM-CM6-1-HR	29	KIOST-ESM
10	CNRM-ESM2-1	30	MCM-UA-1-0
11	CanESM5	31	MIROC-ES2L
12	CanESM5-CanOE	32	MIROC6
13	EC-Earth3	33	MPI-ESM1-2-HR
14	EC-Earth3-CC	34	MPI-ESM1-2-LR
15	EC-Earth3-Veg	35	MRI-ESM2-0
16	EC-Earth3-Veg-LR	36	NESM3
17	FGOALS-f3-L	37	UKESM1-0-LL
18	GFDL-CM4		
19	GFDL-ESM4		
20	GISS-E2-1-G		

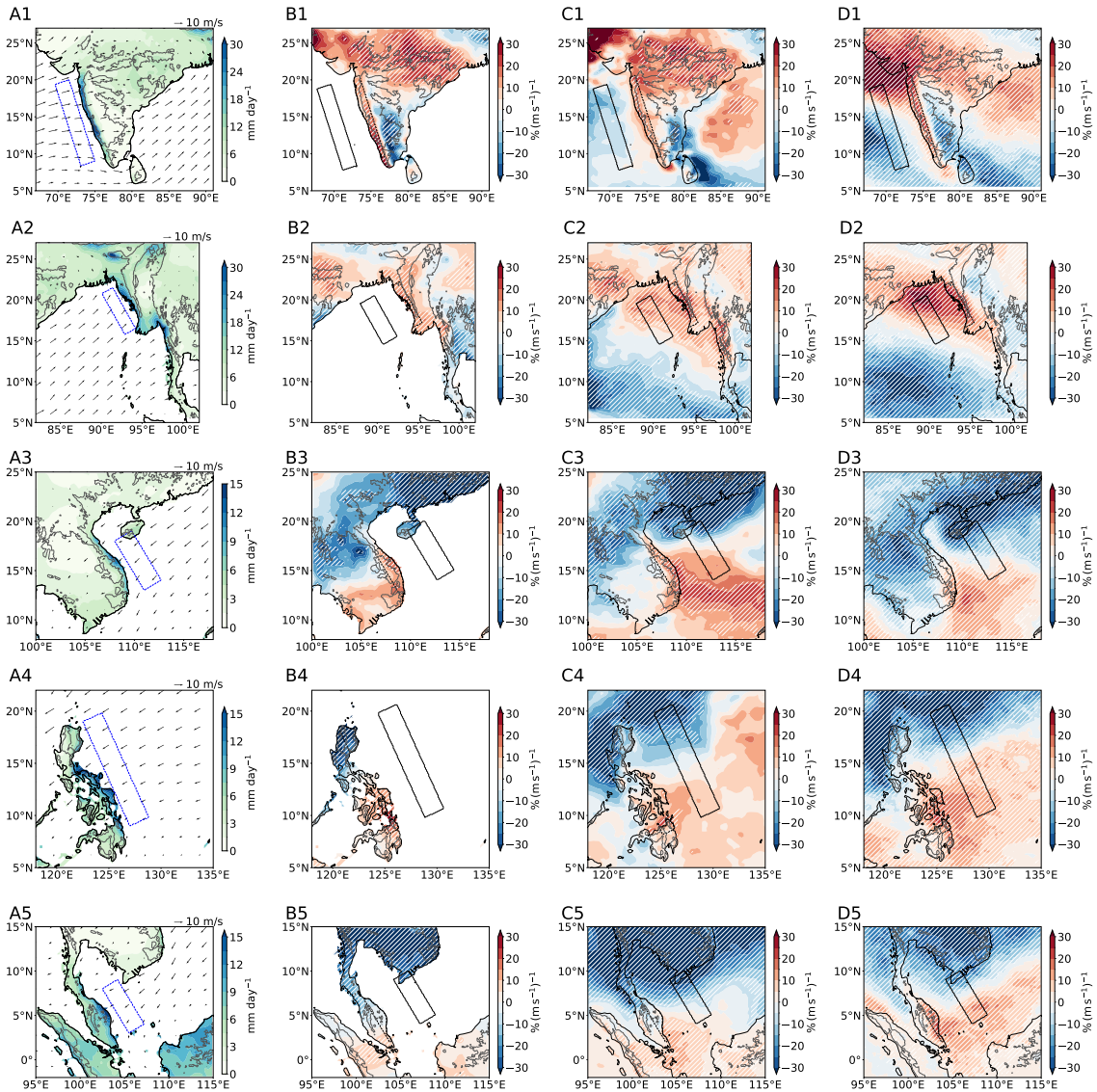


Figure S1. Mean precipitation and winds, and spatial patterns of rainfall scaling rates in five regions at multiple time scales. (A1 - A5) Seasonal mean (1960-2015) APHRODITE precipitation and 100 m winds from ERA5 in each region. See Appendix B for the rainy seasons considered. Gray contours indicate the 500 m surface height level. (B1 - B5) Sensitivity of seasonal-mean APHRODITE precipitation to cross-slope wind speed upstream of each region. Regions hatched in white satisfy the false discovery rate criterion with $\alpha = 0.1$. Winds are averaged in the blue dashed rectangle shown in panel 1 of each row. (C1 - C5) As in (B1 - B5), except ERA5 seasonal-mean precipitation is used. (D1 - D5) As in (B1 - B5), except IMERG daily-mean precipitation is used, and regressions are performed against daily-mean cross-slope wind averaged upstream of each region.

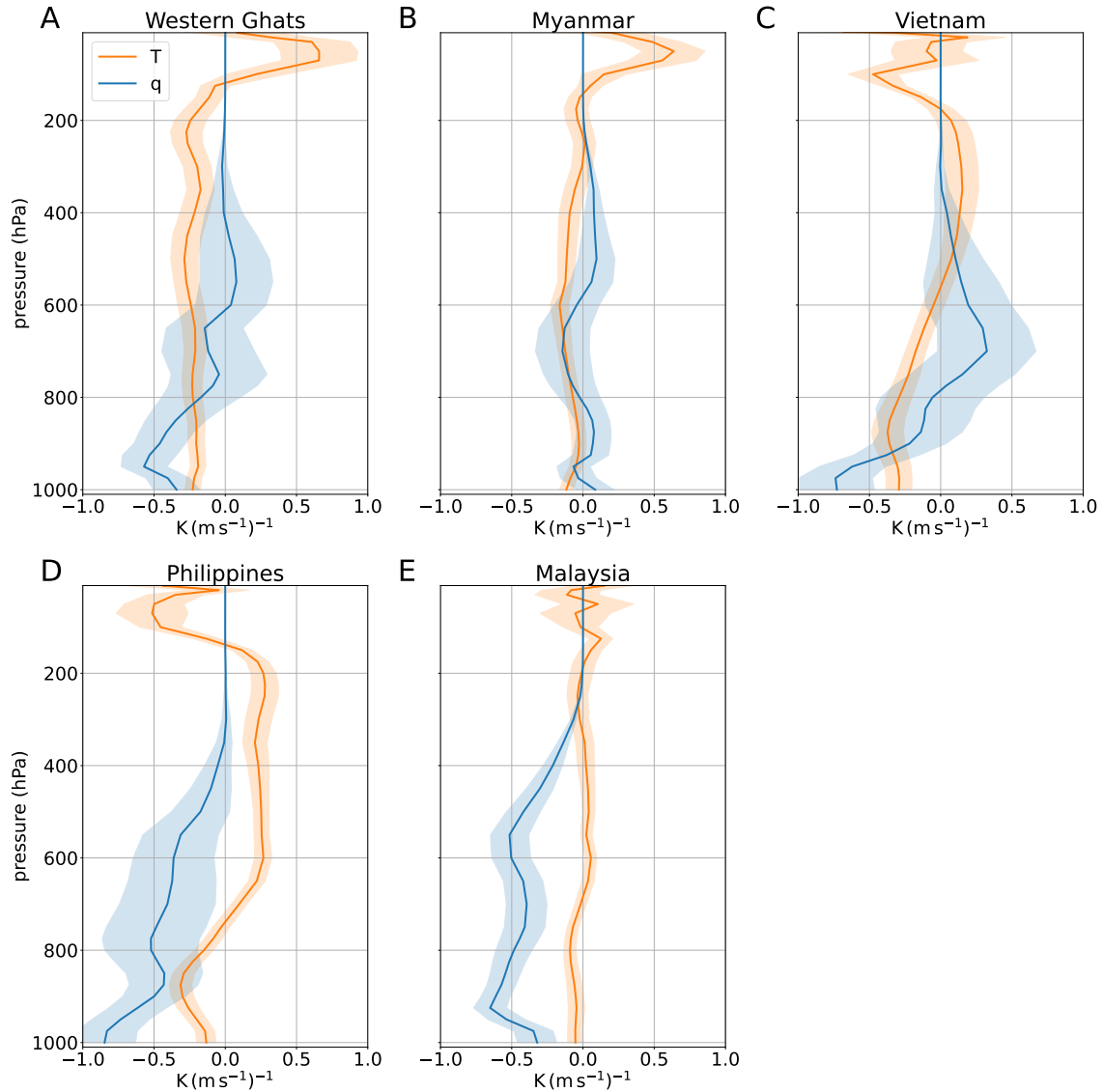


Figure S2. Interannual changes in upstream thermodynamic conditions associated with changes in cross-slope wind. ERA5 seasonal-mean temperature (orange) and moisture (blue) averaged 400 km upstream of each region (solid black boxes in Fig. S1 B1-B5) are regressed against upstream cross-slope wind. Shadings show 95% confidence intervals for each regression slope. Note that upstream of the Philippines and Malaysia, enhanced cross-slope wind is associated with a deep drying pattern. This drying entails a decrease in P_0 , and helps understand why P' scales strongly with U while $P = P_0 + P'$ doesn't.